JCI insight

Reciprocal immune enhancement of dengue and Zika virus infection in human skin

Priscila M. S. Castanha, … , Ernesto T. A. Marques, Simon M. Barratt-Boyes

JCI Insight. 2020;5(3):e133653. https://doi.org/10.1172/jci.insight.133653.

Research Article | Immunology | Infectious disease

Graphical abstract

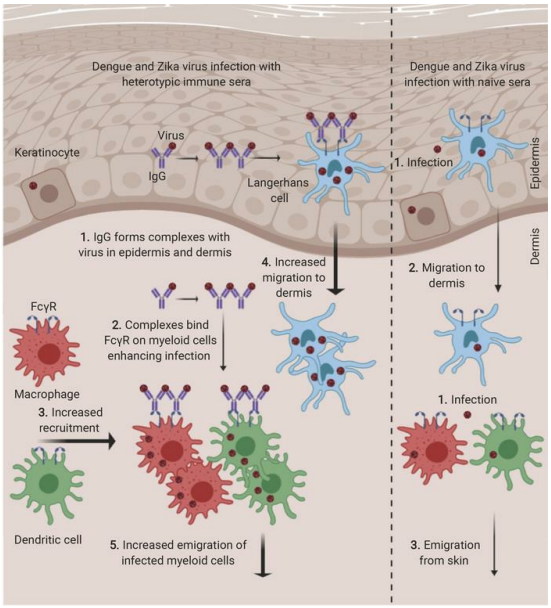

Find the latest version:

https://jci.me/133653/pdf

JCI insight

RESEARCH ARTICLE

Reciprocal immune enhancement of dengue and Zika virus infection in human skin

Priscila M. S. Castanha,[1,2,3] Geza Erdos,[4] Simon C. Watkins,[5,6,7] Louis D. Falo Jr.,[4] Ernesto T. A. Marques,[1,3] and Simon M. Barratt-Boyes[1,7]

[1]Department of Infectious Diseases and Microbiology, University of Pittsburgh, Pittsburgh, Pennsylvania, USA. [2]Biological Science Institute and Faculty of Medical Science, University of Pernambuco, Recife, Brazil. [3]Aggeu Magalhães Institute, Oswaldo Cruz Foundation, Recife, Brazil. [4]Department of Dermatology, [5]Center for Biologic Imaging, [6]Department of Cell Biology, and [7]Department of Immunology, University of Pittsburgh, Pittsburgh, Pennsylvania, USA.

Dengue virus (DENV) and Zika virus (ZIKV) are closely related mosquito-borne flaviviruses that co-circulate in tropical regions and constitute major threats to global human health. Whether preexisting immunity to one virus affects disease caused by the other during primary or secondary infections is unknown but is critical in preparing for future outbreaks and predicting vaccine safety. Using a human skin explant model, we show that DENV-3 immune sera increased recruitment and infection of Langerhans cells, macrophages, and dermal dendritic cells following inoculation with DENV-2 or ZIKV. Similarly, ZIKV immune sera enhanced infection with DENV-2. Immune sera increased migration of infected Langerhans cells to the dermis and emigration of infected cells out of skin. Heterotypic immune sera increased viral RNA in the dermis almost 10-fold and reduced the amount of virus required to infect a majority of myeloid cells by 100- to 1000-fold. Enhancement was associated with cross-reactive IgG and induction of IL-10 expression and was mediated by both CD32 and CD64 Fcγ receptors. These findings reveal that preexisting heterotypic immunity greatly enhances DENV and ZIKV infection, replication, and spread in human skin. This relevant tissue model will be valuable in assessing the efficacy and risk of dengue and Zika vaccines in humans.

Introduction

Dengue is the most important mosquito-transmitted viral disease worldwide, with recent estimates indicating that 390 million infections and 96 million symptomatic dengue cases occur annually (1). Infection by any of the 4 dengue virus (DENV) serotypes (DENV-1–4) can result in a wide spectrum of clinical manifestations, ranging from asymptomatic infection or flu-like febrile illness to life-threatening, severe dengue during primary or secondary infections (2). Zika virus (ZIKV) is a closely related flavivirus that has spread rapidly in the Americas and is associated with devastating clinical consequences in affected individuals, including congenital malformations and autoimmune polyneuropathy (3, 4). The overlapping spread of ZIKV in DENV-endemic areas raises concerns that interplay between the 2 viruses could alter infection and disease dynamics (5). This is particularly a concern because DENV and ZIKV have a high degree of structural homology (6, 7), and immune responses raised against one virus could affect subsequent infection with the heterologous virus.

Preexisting immunity is a major risk factor for severe dengue because primary DENV infection commonly results in self-limiting febrile illness, whereas secondary DENV infection is more likely to promote severe clinical symptoms (8). Severe dengue also accompanies primary infections in infants born to dengue-immune mothers (9). In vitro, non-neutralizing antibodies bind to DENV, creating immune complexes that are presented to myeloid cells or other cells with Fcγ receptors, resulting in increased production of virus, a phenomenon known as antibody-dependent enhancement (ADE) (8, 10, 11). Mechanistic studies in mice support the role of ADE in increasing infection and disease during DENV infection (12–14). Epidemiologic studies support the relationship between preexisting DENV-binding antibodies and severity of disease during natural DENV infection of humans (15, 16).

The interaction between DENV and ZIKV is less understood. Enhancement of ZIKV infection with DENV-specific antibodies and immune serum has been demonstrated by in vitro and murine studies (17–21). However, whether preexisting immunity to DENV alters the pathogenesis of ZIKV infections in humans, particularly as immunity wanes, is unclear. Conversely, studies in macaques suggest that preexist-

Conflict of interest: GE and LDF are inventors on an issued patent (US 8,834,423 B2; US 9,944,019 B2; US 10,441768 B2) through the University of Pittsburgh for microneedle array technology.

Submitted: September 26, 2019
Accepted: December 30, 2019
Published: February 13, 2020.

Reference information: *JCI Insight*. 2020;5(3):e133653. https://doi.org/10.1172/jci.insight.133653.

ing immunity to ZIKV enhances DENV replication (22), but whether this occurs in humans is unknown. These are critical issues not only for understanding the epidemiology of natural infections but also for vaccine safety because vaccination against DENV or ZIKV could exacerbate disease following subsequent infection with the heterologous flavivirus (23).

DENV and ZIKV undergo primary replication in skin after inoculation by an infected mosquito, and the skin is rich in myeloid cells, including Langerhans cells (LCs), macrophages, and dermal dendritic cells (DCs), which are susceptible to infection with either virus (24–28). These factors suggest that the skin is a principal site for enhancement of DENV and ZIKV infection immediately following transmission leading to increased virus spread in the host.

We adapted an established ex vivo model of DENV infection of human skin (25) to determine whether preexisting immunity to DENV or ZIKV enhanced infection with heterologous virus, using small volumes of monotypic immune human sera introduced via microneedle arrays. Our findings reveal that cross-reactive antibodies within immune serum greatly exacerbate infection and spread of both DENV and ZIKV in human skin, primarily within the dermis. Enhancement of infection was associated with increased recruitment, infection, and migration of LCs, macrophages, and dermal DCs and was completely blocked by neutralizing antibodies against both CD64 and CD32 Fcγ receptors. These data have important implications for the impact of both naturally acquired and vaccine-acquired immunity to DENV and ZIKV on humans living in or visiting dengue- and Zika-endemic regions.

Results

Immunity to DENV-3 potently enhances infection with DENV-2 in human skin. To investigate the potential for preexisting immunity to alter flavivirus infection dynamics in human skin, we first evaluated crosstalk between 2 DENV serotypes. We formulated dissolvable microneedle arrays to contain 10-fold dilutions of pooled sera from healthy individuals in Brazil who had previously experienced primary infection with DENV-3. Sera were confirmed to have neutralizing antibodies against DENV-3 but against no other DENV serotype or related flaviviruses, including ZIKV, yellow fever, and West Nile viruses (Table 1)(29, 30). Microneedle arrays containing pooled flavivirus-naive sera were prepared in a similar fashion and used as controls. Individual arrays were manually applied to the middle of 1-in.^{2} pieces of abdominal skin obtained by elective plastic surgery. Skin was incubated with arrays for 15 minutes to allow needle tips to dissolve, delivering a 1- to 2-μL volume to the central area of skin. One thousand focus-forming units (FFU) of DENV was then inoculated into skin using a bifurcated needle (25). This quantity of virus approximates physiologic levels of virus that would be transmitted by the bite of an infected mosquito (31). Skin explants were harvested 24 hours after inoculation and stained with antibody against DENV nonstructural protein 3 (NS3), which is expressed only during virus replication.

We first examined the effect of immune sera on infection with the homologous DENV-3 (strain Philippines/H87/1956). In the presence of naive sera, NS3 expression was detected in cells in the epidermis and dermis, and the extent of infection was independent of serum dilution, as determined by quantitative image analysis (Figure 1, A and B). As expected, inoculation of DENV-3 into skin pretreated with DENV-3 immune sera resulted in a dose-dependent inhibition of virus replication, reaching more than 80% inhibition in the dermis at the highest serum concentration of 1:40 (Figure 1, A and B). Inoculating DENV-2 (strain Thailand/16681/1964) into skin that was pretreated with naive sera resulted in NS3 expression in both the epidermis and dermis, similar to that seen with DENV-3. In marked contrast, infection with DENV-2 in skin pretreated with DENV-3 immune sera resulted in a substantial increase in infected cells in a dose-dependent manner. This effect was most pronounced in the dermis, where the density of DENV-2–infected cells increased more than 3-fold at a 1:40 dilution of immune sera (Figure 1, A and B). We repeated this experiment using increasing amounts of DENV-2 in the presence of naive serum. Similar levels of infection of cells in the dermis occurred when 10^5 to 10^6 FFU of DENV-2 was inoculated with naive sera as with 10^3 FFU DENV-2 and DENV-3 immune sera (Figure 1C). Thus, the presence of DENV-3 immune sera required 100 to 1000 times less DENV-2 to produce the same degree of infection as virus alone. We then quantified DENV genomes by quantitative real-time PCR at 24 hours after infection with 10^3 FFU of DENV-2 after enzymatic separation of the epidermis and dermis. At a 1:40 dilution of immune or naive sera, no difference in virus RNA was observed in the epidermis, consistent with our imaging data indicating minimal enhancement within this compartment. However, in the dermis the presence of DENV-3 immune sera increased viral RNA by approximately 10-fold relative to DENV-2 alone (Figure 1D).

Table 1. Neutralizing antibody titers of DENV-3 and ZIKV immune sera

	Reciprocal neutralizing antibody titer[A]				
Subject	**DENV-1**	**DENV-2**	**DENV-3**	**DENV-4**	**ZIKV**
DENV-3 immune sera					
B034	<20	<20	380	<20	<20
B113	<20	<20	375	<20	<20
B116	<20	<20	389	<20	<20
B182	<20	<20	1221	<20	<20
B198	<20	<20	341	<20	<20
B212	<20	<20	1282	<20	<20
B380	<20	<20	1320	<20	<20
Mean	<20	<20	758	<20	<20
ZIKV immune sera					
01-007-2-2	<20	<20	<20	<20	140
01-008-2-2	<20	<20	<20	<20	277
01-009-2-2	<20	<20	<20	<20	529
03-006-2-2	<20	<20	<20	<20	673
IAM 1	<20	<20	<20	<20	2560
IAM 5	<20	<20	<20	<20	12,980
IAM 11	<20	<20	<20	<20	634
IAM 23	<20	<20	<20	<20	573
Mean	<20	<20	<20	<20	2296

[A]Determined by plaque reduction neutralization test.

DENV-3 immune serum increases recruitment and infection of dermal macrophages and DCs in skin inoculated with DENV-2. To examine the role of myeloid cells in enhancement of DENV infection in skin, we quantified the density of macrophages and DCs in the dermis after inoculation with 10^3 FFU of DENV-2 in the presence or absence of DENV-3 immune sera. DENV-2 alone resulted in increased density of $CD163^+$ macrophages and $CD1c^+$ dermal DCs relative to mock-infected skin, as we have previously described (Figure 2, A and B) (25). However, DENV-3 immune sera increased the density of macrophages and dermal DCs by 2- to 3-fold over DENV-2 alone (Figure 2, A and B). To determine whether proliferation of myeloid cells within the dermis accounted for this increased density, we stained sections with antibody against the nuclear antigen Ki-67, which is expressed in recently divided cells. No Ki-67–expressing cells were identified in the dermis regardless of condition (Supplemental Figure 1; supplemental material available online with this article; https://doi.org/10.1172/jci.insight.133653DS1). These data indicate that macrophages and DCs were recruited locally to the foci of infection in increased numbers in the presence of DENV-3 immune sera. In addition, DENV-3 immune sera increased the density of dermal DCs and macrophages that were infected by 4- to 6-fold relative to naive sera. Infection of macrophages and DCs reached 50% to 65% of their respective populations at the highest serum concentration (Figure 2, C and D).

DENV-3 immune serum enhances migration and infection of LCs. We next explored the apparent lack of enhancement of DENV-2 infection in the epidermis in the presence of DENV-3 immune sera. We first quantified the density of LCs, the principal myeloid cell in the epidermis, in the presence of immune or naive sera followed by DENV-2 infection. Notably, large cords of $NS3^+CD207^+$ LCs were evident within the dermis of skin inoculated in the presence of DENV-3 immune sera that were absent with naive sera (Figure 3A). At a dilution of 1:40, DENV-3 immune sera increased the density of LCs in the dermis by 5-fold relative to naive sera and concurrently decreased LC density in the epidermis. Eighty percent of LCs that had migrated to the dermis were infected with virus (Figure 3B). There was also a 3-fold increase in the total number of cells in media, indicating that heterologous immune sera augments cell emigration out of skin (Figure 3C). Quantitative real-time PCR demonstrated the presence of significantly more DENV genomes in migrated cells from skin infected with DENV-2 in the presence of DENV-3 immune sera, indicating that migrating cells also harbored more virus (Figure 3D).

We next examined the impact of DENV-3 immune sera on DENV-2 infection of keratinocytes, the most abundant cell type in the epidermis that is among the earliest and most significant targets of DENV infection

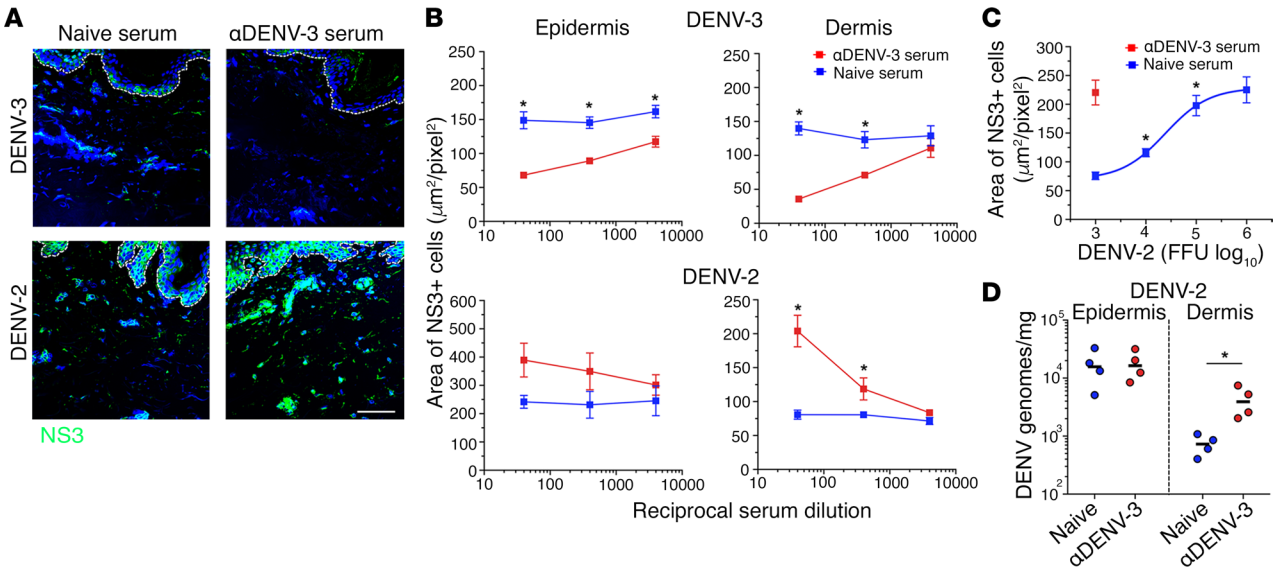

Figure 1. DENV-3 immune sera blocks infection with DENV-3 but enhances infection with DENV-2 in human skin. (**A**) Representative images showing NS3 expression (green) 24 hours after inoculation with 10^3 FFU of DENV-2 or DENV-3 in human skin pretreated with pooled DENV-3 immune sera or naive sera. Blue staining represents nuclei and dotted lines indicate epidermal-dermal junction. Scale bar 50μm. (**B**) Quantification of virus infection in the epidermis and dermis expressed as area of NS3-expressing cells. (**C**) Quantification of infection after inoculation of skin with increasing amounts of DENV-2 in the presence of naive sera or 10^3 FFU of DENV-2 in the presence of DENV-3 immune sera. Data are from 4 skin donors expressed as mean ± SEM. (**D**) Viral RNA copies/mg of tissue in the epidermis and dermis of skin infected with DENV-2 in the presence of DENV-3 immune sera or naive sera. Each symbol is an individual donor and horizontal line is the mean. *$P < 0.05$ (Mann-Whitney U test) comparing immune sera to naive sera at the same dilution.

in human skin (25). Inoculating DENV-3 in skin pretreated with DENV-3 immune sera resulted in reduced infection of keratinocytes, as expected (Figure 3, E and F). Notably, however, neither the density nor proportion of infected keratinocytes was affected by the presence of DENV-3 immune sera (Figure 3, E and F). Thus, heterologous immune serum enhances infection and migration of LCs but has no effect on keratinocytes.

Reciprocal immune enhancement of DENV and ZIKV infection in human skin. We next sought to investigate the potential of monotypic DENV immune sera to enhance ZIKV infection in human skin and vice versa. We inoculated 10^3 FFU of ZIKV (strain H/Brazil/PE243/2015) into skin pretreated with either naive or DENV-3 immune sera. ZIKV replication identified by NS3 staining was seen in the epidermis and to a lesser extent in the dermis in the presence of naive sera (Figure 4, A and B). In contrast, inoculation of ZIKV into skin pretreated with DENV-3 immune sera at the highest concentration more than doubled the density of infected cells in the dermis relative to naive sera, while having no effect on infection in the epidermis (Figure 4, A and B). ZIKV inoculated with DENV-3 immune sera markedly increased the density of LCs in the dermis relative to naive sera (Figure 4C). Moreover, DENV-3 immune sera increased both the density and percentage of ZIKV-infected LCs, DCs, and macrophages within the dermis (Figure 4C).

We next examined the reciprocal effect of ZIKV immune sera on infection with DENV-2. We inoculated 10^3 FFU of ZIKV or DENV-2 into skin pretreated with either naive sera or pooled sera from individuals confirmed to have neutralizing antibodies against ZIKV but not DENV (Table 1). ZIKV immune sera significantly blocked infection with ZIKV in the epidermis and dermis, as expected (Figure 4, D and E). Inoculating DENV-2 in the presence of naive or ZIKV immune sera resulted in similar levels of NS3 expression in cells in the epidermis (Figure 4, D and E). In marked contrast, ZIKV immune sera increased the density of DENV-2–infected cells in a dose-dependent manner within the dermis (Figure 4, D and E). This effect was most pronounced at lower concentrations of ZIKV immune sera (1:400 and 1:4000). To provide an overall comparison between the enhancing effects of heterologous sera on infection with DENV and ZIKV, we calculated the power of enhancement, which is the ratio of the peak number of infected cells in the dermis in the presence of heterotypic serum relative to naive serum. The power of enhancement of preexisting heterotypic immune serum was remarkably similar for both DENV-2 and ZIKV infection at between 2 and 3 (Figure 4F).

Cross-reactive serum antibodies mediate ADE through CD32 and CD64 Fcγ receptor engagement and IL-10 secretion. To determine the factors that mediate the exacerbation of DENV and ZIKV infection in human skin that was driven by heterologous immune serum, we first assessed the capacity for immune sera to bind DENV and

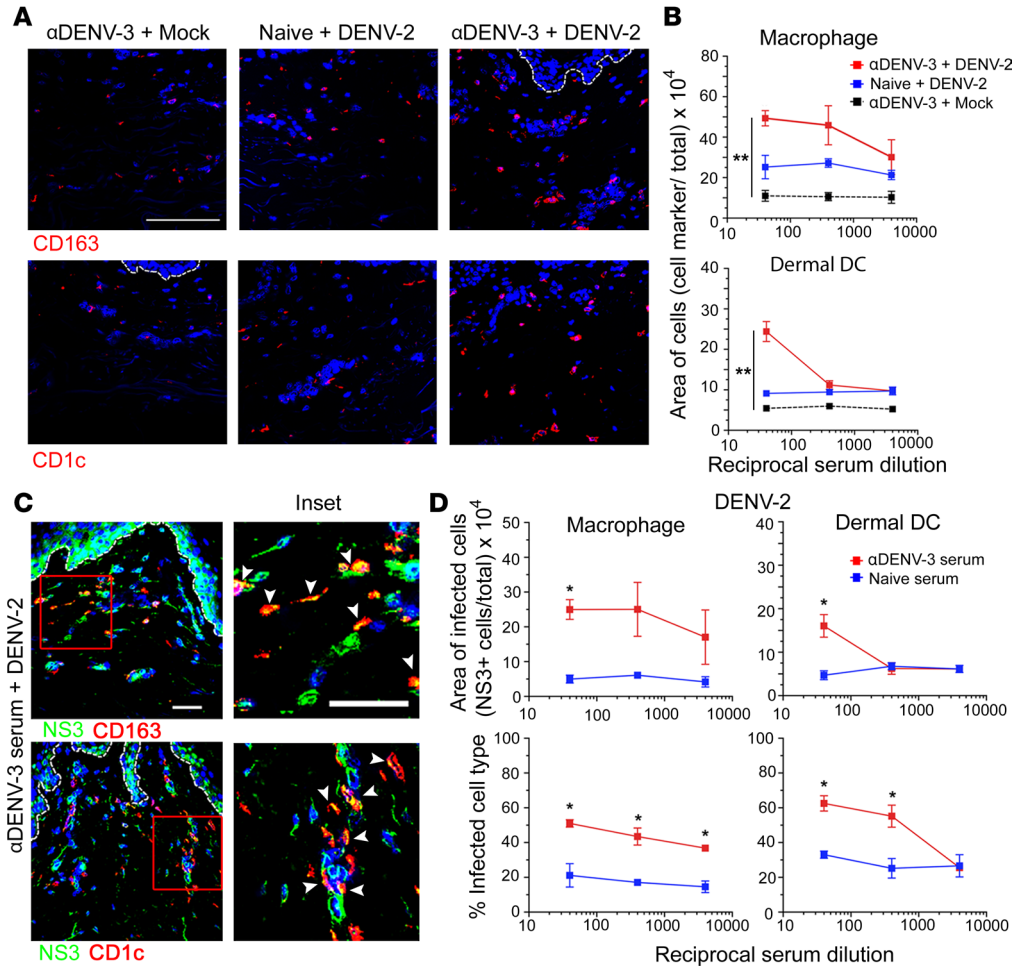

Figure 2. DENV-3 immune sera increases recruitment and infection of macrophages and dermal DCs in skin inoculated with DENV-2. (**A**) Immunofluorescence in the dermis stained with antibodies against CD163 (macrophages, red) and CD1c (dermal DCs, red) after mock infection or inoculation with 10^3 FFU of DENV-2 in the presence of DENV-3 immune sera or naive sera. Scale bar 50μm. (**B**) Quantification of the density of macrophages and dermal DCs in the dermis under different conditions. Data are from 4 skin donors and expressed as mean ± SEM. $^{**}P < 0.01$ determined by Kruskal-Wallis 1-way ANOVA followed by Dunn's multiple-comparisons test. (**C**) Representative images showing staining with antibodies against CD163 or CD1c (red) and NS3 (green) in the dermis of skin infected with DENV-2 in the presence of DENV-3 immune sera. Arrowheads indicate infected cells. Scale bar: 25 μm. Blue staining in **A** and **C** represent nuclei and dotted lines indicate epidermal-dermal junction. (**D**) Quantification of area of infection and percentage of infection for each cell type. Data are from 4 skin donors expressed as mean ± SEM.$^{*}P < 0.05$ (Mann-Whitney *U* test) comparing immune sera to naive sera at the same dilution.

ZIKV particles in an in vitro IgG binding assay. As expected, the IgG in DENV-3 and ZIKV immune sera strongly bound homologous DENV-3 and ZIKV, respectively, in a dose-dependent manner. However, both DENV-3 and ZIKV immune sera also exhibited significant IgG binding to the heterologous viruses when compared with naive sera (Figure 5A). To quantify binding, we calculated the IC_{50}, which is the concentration of IgG that results in 50% binding to virus particles. DENV-3 immune sera bound DENV-3 and DENV-2 particles with similar efficiency, having IC_{50} values of 3.23 and 3.05 $\log_{10}$, respectively, but had lower binding efficiency to ZIKV (1.81 $\log_{10}$). Similarly, ZIKV immune sera bound both DENV serotypes with near equal efficiency (1.77 $\log_{10}$ for DENV-2, 1.52 $\log_{10}$ for DENV-3), although this was weaker than binding to homologous ZIKV (2.06 $\log_{10}$, Supplemental Table 1). Overall, based on endpoint titer, 80% and 60% of binding IgG in DENV-3 immune sera was cross-reactive with DENV-2 and ZIKV, respectively, whereas 80% of binding IgG in ZIKV immune sera was cross-reactive with both DENV-2 and DENV-3 (Figure 5B and Supplemental Figure 2).

We next addressed potential mechanisms of ADE within skin. To determine whether differential cytokine expression contributed to enhanced myeloid cell recruitment and infection, we carried out quantitative real-time PCR analysis for gene expression of a panel of cytokines and chemokines known to be

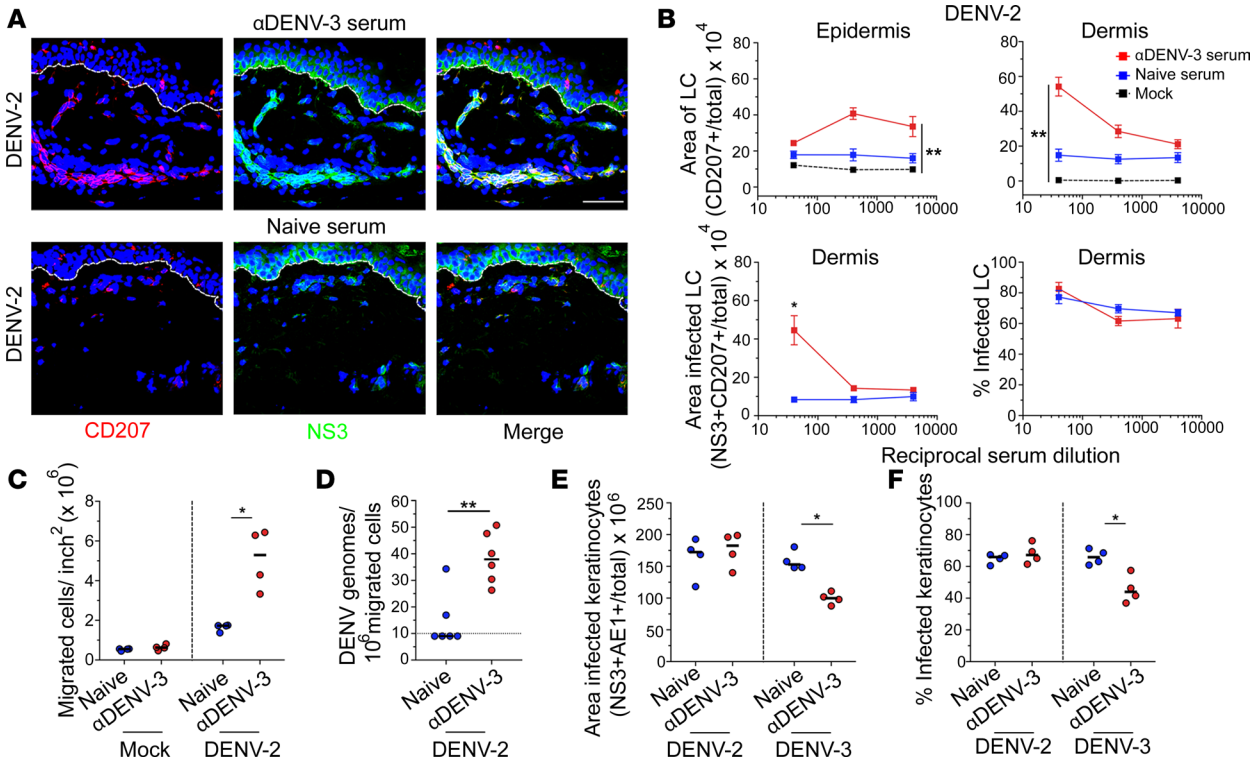

Figure 3. DENV-3 immune sera enhances migration of infected LCs from the epidermis to dermis in skin inoculated with DENV-2. (**A**) Immunofluorescence of skin stained with antibodies against CD207 (LCs, red) and NS3 (green) after inoculation with 10^3 FFU of DENV-2 in skin pretreated with DENV-3 immune sera or naive sera. Blue staining represents nuclei and dotted lines indicate epidermal-dermal junction. Scale bar: 50 μm. (**B**) Quantification of the area of LCs and the area and percentage of infected LCs in the epidermis and dermis. Data are from 4 skin donors expressed as mean ± SEM. $^*P < 0.05$ (Mann-Whitney *U* test) comparing immune sera with naive sera at the same dilution. $^{**}P < 0.01$ determined by Kruskal-Wallis 1-way ANOVA followed by Dunn's multiple-comparisons test. (**C**) Number of migrated cells collected from medium per square inch of skin after DENV-2 or mock infection in the presence of DENV-3 immune sera or naive sera. (**D**) Viral RNA copies/10^6 migrated cells from skin inoculated with DENV-2 in the presence of DENV-3 immune sera or naive sera. Dotted line indicates limit of detection. (**E** and **F**) Quantification of area of infected keratinocytes (**E**) and percentage of infected keratinocytes (**F**) in the epidermis of skin after DENV-2 or mock infection in the presence of DENV-3 immune sera or naive sera. Each symbol is an individual donor and horizontal line is the mean. $^*P < 0.05$, and $^{**}P < 0.01$ (Mann-Whitney *U* test).

involved in skin inflammatory responses. Inoculation of 10^3 FFU of DENV-2 alone induced expression of IL-1β and CCL20, consistent with our previous findings (Figure 5C) (25). However, when DENV-2 was inoculated into skin pretreated with DENV-3 immune sera, there was a strong increase in IL-10 expression (median fold change: 4.11 $\log_2$; range: 3.19–5.58) as compared with naive serum (median fold change: –0.97 $\log_2$; range: –0.33–0.85; Mann-Whitney *U*: 0.028). To determine the role of Fcγ receptors (FcγRs) in the observed increase in virus replication in the presence of immune serum, we next formulated dissolvable microneedle arrays containing neutralizing antibodies against CD32 (FcγRIIa) or CD64 (FcγRI) combined with a 1:40 dilution of immune or naive sera. Individual arrays were applied to the skin before inoculation of 10^3 FFU of DENV-2. Quantitative image analysis revealed no effect of blocking antibodies on infection of cells in the epidermis, as expected (Supplemental Figure 3). In contrast, inoculating DENV-2 in skin pretreated with neutralizing antibodies against CD32 or CD64 combined with DENV-3 immune sera resulted in an 80% reduction in enhancement of infection in the dermis, and antibodies against both receptors fully eliminated enhancement induced by heterotypic immune sera (Figure 5D). Similarly, blocking both CD32 and CD64 inhibited the increase in cell migration out of skin induced by heterotypic immune sera (Figure 5E). Microneedle arrays containing neutralizing antibodies against CD32 or CD64 profoundly reduced both recruitment and infection of macrophages, DCs, and LCs in the dermis relative to isotype control antibody, with a combination of blocking antibodies against both CD32 and CD64 completely eliminating the enhancing effect of immune sera on infection of each cell type (Figure 5, F and G). Collectively, these data indicate that ADE of DENV infection of myeloid cells in the human dermis is a function of both CD64 and CD32 receptors.

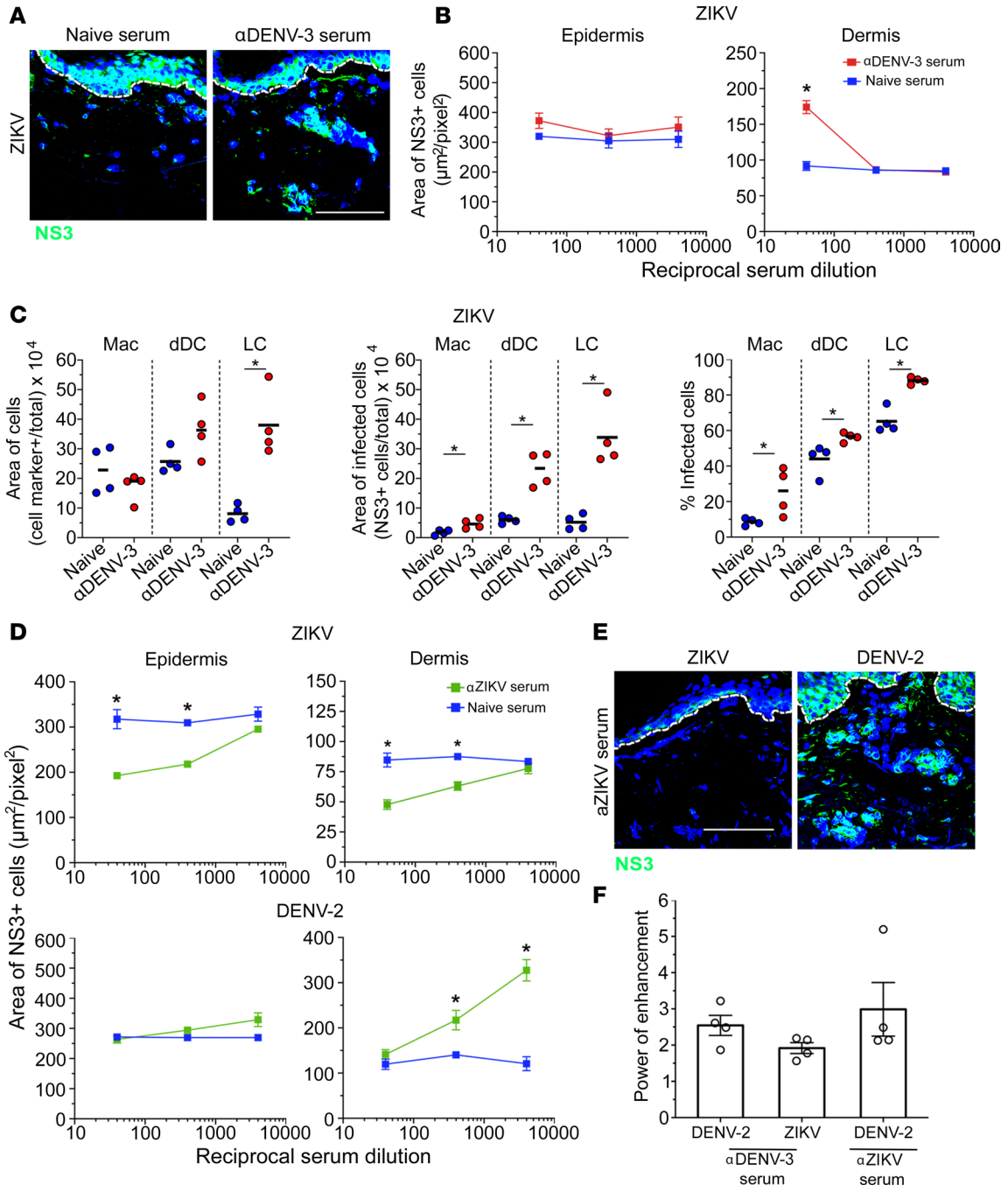

Figure 4. Reciprocal immune enhancement of DENV and ZIKV infection in human skin. (**A**) Representative images showing NS3 (green) expression after inoculation with 10^3 FFU of ZIKV in human skin pretreated with DENV-3 immune sera or naive sera. Scale bar: 50 μm. (**B**) Quantification of ZIKV infection in the epidermis and dermis of skin inoculated in the presence of DENV-3 immune sera or naive sera. *$P < 0.05$ (Mann-Whitney *U* test) comparing DENV-3 immune sera with naive sera. (**C**) Quantification of area of cells, area of infected cells, and percentage of infected cells for each cell type (macrophages, dermal DCs, and LCs) in the dermis after inoculation with ZIKV in skin pretreated with 1:40 dilution of DENV-3 immune sera or naive sera. Each symbol is an individual donor and horizontal line is the mean. *$P < 0.05$ (Mann-Whitney *U* test). (**D**) Quantification of ZIKV and DENV-2 infection in the epidermis and dermis of skin inoculated in the presence of ZIKV immune sera or naive sera. *$P < 0.05$ (Mann-Whitney *U* test) comparing ZIKV immune sera with naive sera. Data in **B** and **D** are from 4 skin donors expressed as mean ± SEM. (**E**) Representative images showing NS3 (green) expression after inoculation with 10^3 FFU of DENV-2 or ZIKV in human skin pretreated with ZIKV immune sera. Scale bar: 50 μm. Blue staining in **A** and **E** represents nuclei and dotted lines indicate epidermal-dermal junction. (**F**) Fold increase (power of enhancement) in the density of DENV-2– and ZIKV-infected cells in the presence of DENV-3 immune sera relative to naive sera and DENV-2–infected cells in the presence of ZIKV immune sera relative to naive sera at peak enhancement. Data are from 4 skin donors expressed as mean ± SEM.

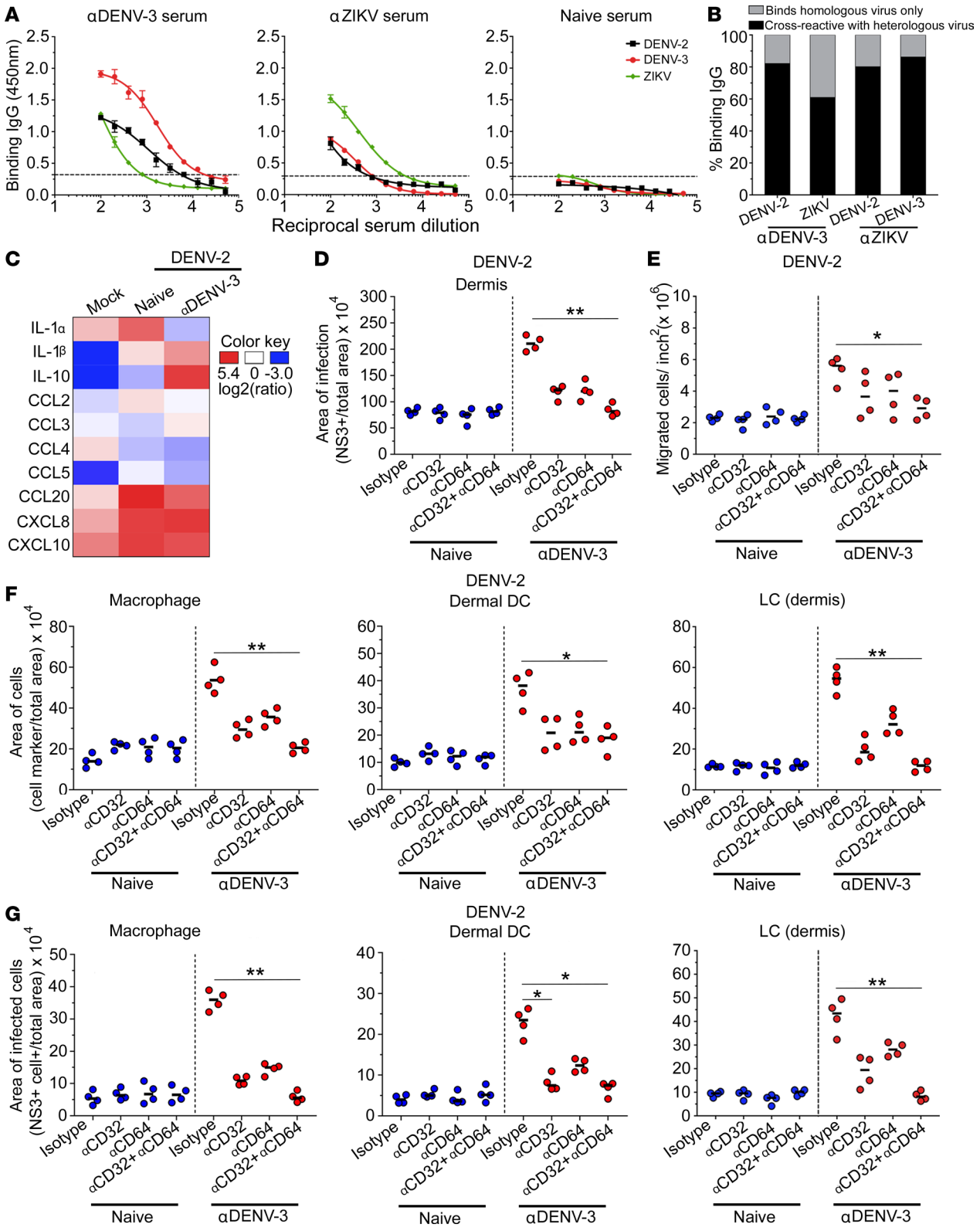

Figure 5. Cross-reactive antibodies in immune sera mediate enhancement through CD32 and CD64 Fcγ receptor engagement and IL-10 expression. (**A**) Binding IgG properties of DENV-3 and ZIKV immune serum to DENV-2, DENV-3, and ZIKV particles. Data are from 4 skin donors expressed as mean ± SEM. Dotted line represents optical density value of the negative control plus 3 times the standard deviation. (**B**) Percentage of binding IgG in immune sera that binds to homologous virus or cross-reacts with heterologous virus, calculated as follows: percentage of cross-reactive binding IgG = (endpoint titer against heterologous virus/endpoint titer against homologous virus) × 100. Percentage of type-specific binding IgG = 100 – percentage of cross-reactive IgG. (**C**) Expression of innate immune genes determined by real-time PCR in whole digests of mock-infected skin or skin infected with DENV-2 in the presence of DENV-3 immune sera or naive sera. Changes in expression of genes are presented as a heatmap of $\log_2$-transformed expression ratios relative to control

skin before infection. (**D**) Quantification of the density of NS3-expressing cells in the dermis after inoculation with 10^3 FFU of DENV-2 in skin pretreated with neutralizing antibodies against CD32 or CD64 combined with a 1:40 dilution of DENV-3 immune sera or naive sera. (**E**) Number of migrated cells collected from medium per square inch of skin treated as in **D**. (**F**) Quantification of the density of macrophages, dermal DCs, and LCs in the dermis after inoculation with DENV-2 in skin treated as in **D**. (**G**) Quantification of the area of infected macrophages, dermal DCs, and LCs in the dermis after inoculation with DENV-2 in skin treated as in **D**. Data are from 4 skin donors expressed as mean ± SEM. $*P < 0.05$, and $**P < 0.05$ determined by Kruskal-Wallis 1-way ANOVA followed by Dunn's multiple-comparisons test.

Discussion

Our findings reveal for the first time to our knowledge that cross-reactive antibodies in human immune serum markedly exacerbate infection and spread of both DENV and ZIKV in human skin, the primary site of virus transmission. Preexisting immunity increased both the density of infected cells and the amount of virus recovered from the dermis, consistent with other reports using in vitro and murine models (10, 18–20, 32, 33). Strikingly, heterotypic immune serum effectively reduced the amount of virus needed to produce a similar level of infection in naive skin by 100 to 1000 times, such that inoculation of 10^3 FFU, roughly equivalent to the amount of virus delivered by a mosquito (31), infected 50% to 80% of all myeloid cells in the dermis. These data suggest that preexisting heterotypic immunity not only enhances virus replication and spread within human skin but also may increase efficiency of transmission because 1 bite of a single infected mosquito would be sufficient to cause productive infection.

Although DENV and ZIKV replication takes place in both the epidermis and dermis, enhancement of infection by preexisting immunity was restricted to the dermis. Localized recruitment and infection of $CD163^+$ macrophages and $CD1c^+$ dermal DCs clearly contributed to enhancement of infection in the dermis, consistent with studies in IFN-α/β receptor–deficient mice (14). However, a key factor in enhancement of infection in human skin was the 5-fold increase in the number of infected LCs that exited the epidermis, substantially greater than that seen with virus alone (25, 26, 34, 35). Moreover, preexisting immunity increased the number of cells migrating out of skin by the same amount. Our prior studies showed that a significant proportion of migrating cells are LCs, dermal DCs, and macrophages (25), and in the current study, these migrating cells carried more virus when infection occurred in the presence of heterotypic immune sera. These findings indicate that heterotypic immune enhancement of DENV and ZIKV infection in skin would result in increased myeloid cell dissemination of virus in the host (14, 24, 26).

The majority of studies using cell lines and murine models suggest a primary role for CD32 (FcγRIIa) in mediating ADE of DENV and ZIKV infection (19, 36–39). Our data in the ex vivo human skin model indicate that both CD32 and CD64 (FcγRI) contribute substantially to ADE and that blocking both receptors is required to completely eliminate enhancement, consistent with the notion of FcγR synergy in enhancement of flavivirus infection (40). It is likely that in intact human skin ADE is influenced by the ratio of expression levels of CD64 and CD32 on each cell type and on the signaling pathway followed by FcγR cross-linking, which potentially induces unique cell responses (39, 41, 42). Notably, keratinocytes, which lack expression of FcγRs (43, 44), did not have enhanced infection in the presence of heterotypic immune serum, and infection of this cell type was unaffected by blocking antibodies to CD32 and CD64.

Our findings suggest that IL-10 may play an important role in the observed immune enhancement of DENV and ZIKV infection in skin. Although the source of IL-10 in skin needs to be determined, this finding is consistent with previous in vitro studies showing that macrophages and DCs strongly upregulate IL-10 production upon exposure to antibody-opsonized virus in an FcγR-dependent manner. Our findings also are in consonance with epidemiological studies showing higher levels of IL-10 production in patients experiencing secondary DENV infections (32, 39, 45–49). FcγR engagement of immune complexes results in suppression of innate immune responses through both increased IL-10 production and a bias toward a Th2 response, ultimately leading to increased virus output per infected cell (32, 39, 48, 49). Interestingly, we found a 2- to 3-fold increase in the overall number of cells with viral replication in the dermis and a 10-fold increase in virus genome production in skin inoculated with heterotypic antibodies. These findings suggest that both an increased number of infected cells (extrinsic ADE) and an increase in virus output per cell (intrinsic ADE) (50) are active processes in human skin.

Our data indicate that the majority of binding IgG in monotypic DENV-3 and ZIKV human immune serum is in fact cross-reactive with heterologous virus, a critical feature in the observed immune enhancement of both DENV and ZIKV infection in skin. This finding is consistent with previous reports showing that individuals exposed to primary DENV or ZIKV infections develop a dominant flavivirus cross-reactive IgG response

and a minor population of antibodies that are against the virus of infection (10, 51). Notably, despite similar frequencies of cross-reactive binding IgG to DENV-2, peak enhancement of DENV-2 by ZIKV immune serum was observed at substantially lower serum concentrations compared with the peak enhancement by DENV-3 immune serum. Interestingly, one of the earliest prospective studies of ADE in children showed that the relative risk of severe dengue increased 6-fold when in vitro enhancement of infection was induced by high serum concentrations relative to low serum concentrations (11). It is notable that the ZIKV immune sera used in our study were from individuals with very high ZIKV-neutralizing titers, with mean neutralizing titers more than 3-fold higher than the DENV-3 immune sera, but only a fraction of ZIKV-infected individuals generate this level of antibody response. Nevertheless, this finding may suggest that individuals with preexisting immunity to DENV-3 may be at greater risk of disease when infected with heterologous DENV or ZIKV. The data also indicate that a ZIKV vaccine that induces low antibody titers may increase the risk of severe dengue.

It is well described that mosquito saliva enhances infection of a number of arthropod-borne viruses, including DENV (52–55). A recent study using IFN-α/β receptor–deficient mice shows greater recruitment and infection of skin-resident macrophages and DCs after intradermal inoculation of DENV in the presence of enhancing antibodies that depended on mosquito salivary gland components (14). Although serum antibodies normally are present at low concentration in the interstitial space (56), the act of mosquito probing itself induces edema, which traps both virus and plasma in skin (57), and a similar effect is seen with mosquito saliva (14). Thus, it is reasonable to speculate that mosquito inoculation of virus would further intensify the observed enhancement effect in human skin. Additional experiments will be required to test this hypothesis, ideally with DENV- and ZIKV-infected mosquitoes probing skin explants.

In summary, our data using a novel ex vivo system reveal that preexisting immunity to heterologous flavivirus greatly exacerbates DENV and ZIKV infection in human skin, markedly reducing the amount of virus needed to infect myeloid cells while increasing migration of infected cells out of skin. Whether increased dissemination of virus from skin in the presence of heterotypic immune sera leads to more severe clinical disease in the host is not possible to address with this model, although murine studies are consistent with this hypothesis (14). In terms of vaccination, the findings emphasize the absolute need to develop vaccines that elicit an appropriate range of potent, high-affinity, cross-reactive antibodies that neutralize rather than enhance heterologous virus. By determining the effects of vaccine-induced antibodies on virus infection, our model will serve as a valuable tool for assessing vaccine safety and risk.

Methods

Cells and viruses. Vero cells (African green monkey kidney epithelial; ATCC CCL-81) were maintained in Dulbecco's modified Eagle medium (DMEM) supplemented with 10% fetal bovine serum, 2 mM L-glutamine, 1.5 g/L sodium bicarbonate, 100 U/mL penicillin, and 100 μg/mL of streptomycin and incubated at 37°C in 5% CO_2. C6/36 cells (*Aedes albopictus* mosquito cell line; ATCC CRL-1660) were maintained in DMEM supplemented with 10% fetal bovine serum, 2 mM L-glutamine, 1.5 g/L sodium bicarbonate, 100 U/mL penicillin, 100 μg/mL of streptomycin, and 1% tryptose phosphate broth and incubated at 28°C in 5% CO_2. Virus stocks of the prototype DENV-2 (strain Thailand/16681/1964) and DENV-3 (strain Philippines/H87/1956) serotypes were prepared by inoculation onto an 80% confluent monolayer of C6/36 cells. Supernatants were harvested at 7 and 15 days after infection and concentrated by ultracentrifugation before storage at –80°C. DENV titers of the stock were determined via a modified FFU assay using Vero cells (58). Virus stocks of ZIKV (strain Brazil/PE243/2015) were prepared in Vero cells, and virus titer was determined through plaque assay (20).

Immune serum and microneedle arrays. DENV serotype–specific and ZIKV-specific immune human sera were delivered to the skin using tip-loaded dissolvable 3:2 carboxymethyl cellulose/trehalose microneedle arrays fabricated as described (59). Arrays were loaded with 1:40, 1:400, or 1:4000 dilutions of each pooled serum. Serum samples from individuals who experienced a primary DENV-3 infection were collected in a prospective cohort study in Brazil and were confirmed to have solely DENV-3 monotypic immunity by plaque reduction neutralization assay (29). All samples tested positive and negative for anti-DENV IgG and IgM, respectively (anti-DENV IgG indirect ELISA and IgM capture ELISA; PanBio). Pooled sera from individuals who had experienced primary ZIKV infection were collected in epidemiological studies conducted in Brazil (3, 60). Sera were confirmed to have neutralizing antibodies against ZIKV but no other DENV serotype by plaque reduction neutralization assay. Control arrays contained dilutions of flavivirus-naive serum (human serum off clot sterile type AB; MP Biomedicals). For blocking experiments, arrays containing 10 μg of neutralizing antibodies against human CD32 (IV.3, STEMCELL Technologies) or CD64 (10.1; BioLegend) or

isotype control antibodies combined with either DENV-3 immune or flavivirus-naive sera at 1:40 dilution were formulated. The concentration of neutralizing antibodies was twice the neutralization dose required to saturate surface expression of CD32 and CD64 molecules (36, 61) multiplied by a factor of 2.3 to compensate for dilution following dispersal within skin.

Skin processing and virus inoculation. Healthy skin was obtained from 16 White individuals undergoing elective abdominoplasty or panniculectomy surgery. Donors were from the Pittsburgh, Pennsylvania, region, an area with no local transmission of dengue or Zika. Lack of immunity to DENV-1–4 and ZIKV was confirmed by ELISA in 6 individuals from which sera were available. Skin processing was carried out as previously described (25). Briefly, residual adipose tissue was trimmed from the underside of the skin, and tissue was cut into full-thickness 1-in.^{2} explants. Microneedle arrays were manually applied to skin explants for 15 minutes to allow needle tips to dissolve, leaving loading reagents in the skin. Following the removal of arrays, a suspension containing 5×10^3 FFU of virus (50 μL) was placed in the region of array application on the skin surface. Bifurcated skin allergy–testing needles (Röchling Medical) were used to repeatedly puncture the skin surface through the inoculum to deliver virus into the epidermis and dermis. This inoculation method results in the delivery of approximately 10 μL of virus suspension (equivalent to 10^3 FFU of virus) into the skin (25). Inoculated explants were incubated at 37°C in 5% CO_2 for 2 hours. Following incubation, explants were placed dermis-side down on mesh grids or filter paper in tissue culture dishes and incubated at the liquid-air interface in RPMI 1640 complete medium (10% fetal bovine serum, 2 mM L-glutamine, 100 U/mL penicillin, 100 μg/mL of streptomycin, 10mM HEPES, 1% sodium pyruvate, and 1% nonessential amino acids) at 37°C for 24 hours. For immunohistochemistry analysis, inoculated skin was submerged in 30% sucrose overnight at 4°C and then kept at –80°C until sectioned. For quantitative real-time PCR, a 4-mm punch biopsy from inoculated skin was obtained, submerged in Dispase II solution (2.4 U/mL in PBS), and incubated overnight at 4°C. Epidermal sheets were separated from the dermis and both samples immediately subjected to viral RNA isolation.

Immunohistochemistry. Immunohistochemistry was performed as described (25), using the following antibodies: polyclonal rabbit anti–pan DENV NS3 antibody (provided by Sujan Shresta, La Jolla Institute for Allergy and Immunology, San Diego, California, USA), anti–cytokeratin pan type I monoclonal antibody (AE-1; Invitrogen, Thermo Fisher Scientific, MA5-13144), anti-CD163 antibody (5C6-FAT; Novus Biologicals, BM4041), anti-CD207/langerin (DCGM4; Beckman Coulter, IM3449), anti-CD1c antibody (L161; Abcam, ab190305), and anti–Ki-67 antibody (SP-6; Invitrogen, Thermo Fisher Scientific, MA5-14520). Secondary antibodies were from Invitrogen, Thermo Fisher Scientific, and included goat anti–mouse IgG1, Alexa Fluor 546 (A-21123), and donkey anti–rabbit IgG, Alexa Fluor 488 (A-21206).

Quantitative image analysis. Image analysis was performed by thresholding for positive staining and normalizing to total tissue area using Nikon NIS-Elements AR 4.40 software, as previously described (25). Data for each skin explant were collected from a minimum of 15 confocal images taken from 3 skin sections collected from different sites of virus-inoculated skin. Means from each individual were presented as an individual data point, and data are presented for 4 individuals per experiment.

RNA isolation and quantitative real-time PCR. Total RNA was extracted from the epidermal sheet and dermis using RNeasy Mini Kit (Qiagen), following the manufacturer's instructions. RNA samples were reverse-transcribed using the Maxima First-Strand cDNA Synthesis Kit (Thermo Fisher Scientific). To measure virus genomes, quantitative PCR was undertaken using the GoTaq Probe qPCR kit (Promega) with amplification in the Applied Biosystems QuantStudio 6 Flex real-time PCR system (Thermo Fisher Scientific). The following primer sets were used: forward 5′-AAGGACTAGAGGTTAGAGGAGACCC-3′, reverse 5′-CGTTCTGTGCCTGGAATGATG-3′, and probe 5′-FAM-AACAGCATATTGACGCTGGGAGAGACCAGA-BHQ1-3′ (62). Cycling conditions were as follows: 95°C for 2 minutes, followed by 40 cycles of 95°C for 15 seconds and 60°C for 1 minute. DENV genomes were determined by interpolation onto an internal standard curve produced using 10-fold serial dilutions of a synthetic DENV-2 fragment based on the prototype DENV-2 strain 16681 used for infections in skin. Virus titers were expressed as DENV genome equivalents per milligram of tissue or million migrated cells. The amplification of cytokines, chemokines, and reference genes was performed as previously described (25) using Platinum SYBR Green qPCR SuperMix-UDG (Invitrogen, Thermo Fisher Scientific). Quantities of cytokine and chemokine targets were normalized to the corresponding 18S ribosomal RNA levels in the skin tissues.

Binding IgG assays. Sera were tested for binding to DENV-2, DENV-3, and ZIKV using indirect ELISA. Virus antigens (whole virus) were the same as those used to inoculate skin explants. Briefly, high-binding, half-area, 96-well, polystyrene plates (Corning) were coated overnight at 4°C with DENV-2, DENV-3, or

ZIKV diluted in PBS. Plates were blocked with either nonfat dry milk (Blotting Grade Blocker, Bio-Rad) or albumin from bovine serum (MilliporeSigma) at 5% (*w*/*v*) in PBS with 0.1% (*v*/*v*) Tween-20 (PBS-T). Samples were 2-fold serially diluted (starting at 1:100) and added to the plates for 1 hour. Plates were then washed 5 times with PBS-T and incubated for another 1 hour with horseradish peroxidase–linked anti–human IgG (Jackson ImmunoResearch), before developing using SureBlue Reserve TMB Microwell Peroxidase substrate (SeraCare). Endpoint titers and IC_{50} values were calculated using 4-parameter nonlinear regression and determined as the dilution required for the optical density value of the negative control plus 3 times the SD. Using the estimated endpoint titers, the percentages of cross-reactive and type-specific binding IgG against each virus were calculated as follows: (a) % cross-reactive binding IgG = (endpoint titer against heterologous virus/endpoint titer against homologous virus) × 100, and (b) % type-specific binding IgG = 100 − % of cross-reactive IgG.

Statistics. Results from multiple experiments are presented as mean ± SEM. Comparison between 2 groups was performed using unpaired 2-tailed Mann-Whitney *U* test. Kruskal-Wallis 1-way ANOVA followed by Dunn's multiple-comparisons test was used for multiple comparisons. Data were analyzed with Prism software version 7.0a (GraphPad). A *P* value of less than 0.05 was considered significant.

Study approval. Identifiable private information concerning skin donors was not provided, and no interaction or intervention with donors was possible. Thus, the project did not constitute human subject research, and the study was exempted from full review by the Institutional Review Board of the University of Pittsburgh.

Author contributions

PMSC contributed to study design, performed experiments, analyzed data, and wrote the manuscript. GE and LDF generated microneedle arrays and contributed to study design. SCW contributed to confocal microscopy and image quantification. ETAM contributed to study design, provided serum samples, analyzed data, and wrote the manuscript. SMBB contributed to study design, analyzed data, and wrote the manuscript.

Acknowledgments

We thank Parichat Duangkhae for initial work establishing the experimental system used in these studies, Jeffrey Gusenoff and J. Peter Rubin for providing surgical specimens, and staff in the Department of Plastic Surgery at the University of Pittsburgh for coordinating specimen collection and delivery. PMSC was partially supported by a scholarship from the Coordination for the Improvement of Higher Education Personnel, Brazilian Ministry of Education (440891/2016-7, National Postdoctoral Program). This study was supported in part by National Institutes of Health grant R21AI147017 to SMBB.

Address correspondence to: Simon M. Barratt-Boyes, 2133 Public Health Building, 130 De Soto Street, University of Pittsburgh, Pittsburgh, Pennsylvania, 15260, USA. Phone: 412.383.0625; Email: smbb@pitt.edu. Or to: Ernesto T. A. Marques, 2131 Public Health Building, 130 De Soto Street, University of Pittsburgh, Pittsburgh, Pennsylvania, 15260, USA. Phone: 412.648.2052; Email: marques@pitt.edu.

1. Bhatt S, et al. The global distribution and burden of dengue. *Nature*. 2013;496(7446):504–507.
2. Wilder-Smith A, Ooi EE, Horstick O, Wills B. Dengue. *Lancet*. 2019;393(10169):350–363.
3. de Araújo TVB, et al. Association between microcephaly, Zika virus infection, and other risk factors in Brazil: final report of a case-control study. *Lancet Infect Dis*. 2018;18(3):328–336.
4. Cao-Lormeau VM, et al. Guillain-Barré Syndrome outbreak associated with Zika virus infection in French Polynesia: a case-control study. *Lancet*. 2016;387(10027):1531–1539.
5. Rodriguez-Barraquer I, et al. Impact of preexisting dengue immunity on Zika virus emergence in a dengue endemic region. *Science*. 2019;363(6427):607–610.
6. Hasan SS, Sevvana M, Kuhn RJ, Rossmann MG. Structural biology of Zika virus and other flaviviruses. *Nat Struct Mol Biol*. 2018;25(1):13–20.
7. Dai L, et al. Structures of the Zika virus envelope protein and its complex with a flavivirus broadly protective antibody. *Cell Host Microbe*. 2016;19(5):696–704.
8. Guzman MG, Alvarez M, Halstead SB. Secondary infection as a risk factor for dengue hemorrhagic fever/dengue shock syndrome: an historical perspective and role of antibody-dependent enhancement of infection. *Arch Virol*. 2013;158(7):1445–1459.
9. Halstead SB, et al. Dengue hemorrhagic fever in infants: research opportunities ignored. *Emerging Infect Dis*. 2002;8(12):1474–1479.
10. de Alwis R, et al. Dengue viruses are enhanced by distinct populations of serotype cross-reactive antibodies in human immune sera. *PLoS Pathog*. 2014;10(10):e1004386.
11. Kliks SC, Nisalak A, Brandt WE, Wahl L, Burke DS. Antibody-dependent enhancement of dengue virus growth in human monocytes as a risk factor for dengue hemorrhagic fever. *Am J Trop Med Hyg*. 1989;40(4):444–451.

12. Balsitis SJ, et al. Lethal antibody enhancement of dengue disease in mice is prevented by Fc modification. *PLoS Pathog*. 2010;6(2):e1000790.
13. Ng JK, et al. First experimental in vivo model of enhanced dengue disease severity through maternally acquired heterotypic dengue antibodies. *PLoS Pathog*. 2014;10(4):e1004031.
14. Schmid MA, Glasner DR, Shah S, Michlmayr D, Kramer LD, Harris E. Mosquito saliva increases endothelial permeability in the skin, immune cell migration, and dengue pathogenesis during antibody-dependent enhancement. *PLoS Pathog*. 2016;12(6):e1005676.
15. Vaughn DW, et al. Dengue viremia titer, antibody response pattern, and virus serotype correlate with disease severity. *J Infect Dis*. 2000;181(1):2–9.
16. Katzelnick LC, et al. Antibody-dependent enhancement of severe dengue disease in humans. *Science*. 2017;358(6365):929–932.
17. Fowler AM, et al. Maternally acquired Zika antibodies enhance dengue disease severity in mice. *Cell Host Microbe*. 2018;24(5):743–750.e5.
18. Priyamvada L, et al. Human antibody responses after dengue virus infection are highly cross-reactive to Zika virus. *Proc Natl Acad Sci USA*. 2016;113(28):7852–7857.
19. Bardina SV, et al. Enhancement of Zika virus pathogenesis by preexisting antiflavivirus immunity. *Science*. 2017;356(6334):175–180.
20. Castanha PMS, et al. Dengue virus-specific antibodies enhance Brazilian Zika virus infection. *J Infect Dis*. 2017;215(5):781–785.
21. Dejnirattisai W, et al. Dengue virus sero-cross-reactivity drives antibody-dependent enhancement of infection with Zika virus. *Nat Immunol*. 2016;17(9):1102–1108.
22. George J, et al. Prior exposure to Zika virus significantly enhances peak dengue-2 viremia in rhesus macaques. *Sci Rep*. 2017;7(1):10498.
23. Flasche S, et al. The long-term safety, public health impact, and cost-effectiveness of routine vaccination with a recombinant, live-attenuated dengue vaccine (Dengvaxia): a model comparison study. *PLoS Med*. 2016;13(11):e1002181.
24. Cerny D, et al. Selective susceptibility of human skin antigen presenting cells to productive dengue virus infection. *PLoS Pathog*. 2014;10(12):e1004548.
25. Duangkhae P, et al. Interplay between keratinocytes and myeloid cells drives dengue virus spread in human skin. *J Invest Dermatol*. 2018;138(3):618–626.
26. Schmid MA, Harris E. Monocyte recruitment to the dermis and differentiation to dendritic cells increases the targets for dengue virus replication. *PLoS Pathog*. 2014;10(12):e1004541.
27. Wu SJ, et al. Human skin Langerhans cells are targets of dengue virus infection. *Nat Med*. 2000;6(7):816–820.
28. Hamel R, et al. Biology of Zika virus infection in human skin cells. *J Virol*. 2015;89(17):8880–8896.
29. Castanha PM, et al. Placental transfer of dengue virus (DENV)-specific antibodies and kinetics of DENV infection-enhancing activity in Brazilian infants. *J Infect Dis*. 2016;214(2):265–272.
30. Nascimento EJM, et al. Development of antibody biomarkers of long term and recent dengue virus infections. *J Virol Methods*. 2018;257:62–68.
31. Styer LM, Kent KA, Albright RG, Bennett CJ, Kramer LD, Bernard KA. Mosquitoes inoculate high doses of West Nile virus as they probe and feed on live hosts. *PLoS Pathog*. 2007;3(9):1262–1270.
32. Flipse J, Diosa-Toro MA, Hoornweg TE, van de Pol DP, Urcuqui-Inchima S, Smit JM. Antibody-dependent enhancement of dengue virus infection in primary human macrophages; balancing higher fusion against antiviral responses. *Sci Rep*. 2016;6:29201.
33. Goncalvez AP, Engle RE, St Claire M, Purcell RH, Lai CJ. Monoclonal antibody-mediated enhancement of dengue virus infection in vitro and in vivo and strategies for prevention. *Proc Natl Acad Sci USA*. 2007;104(22):9422–9427.
34. Limon-Flores AY, et al. Dengue virus inoculation to human skin explants: an effective approach to assess in situ the early infection and the effects on cutaneous dendritic cells. *Int J Exp Pathol*. 2005;86(5):323–334.
35. Wu SJ, et al. Human skin Langerhans cells are targets of dengue virus infection. *Nat Med*. 2000;6(7):816–820.
36. Boonnak K, Slike BM, Donofrio GC, Marovich MA. Human FcγRII cytoplasmic domains differentially influence antibody-mediated dengue virus infection. *J Immunol*. 2013;190(11):5659–5665.
37. Boonnak K, et al. Role of dendritic cells in antibody-dependent enhancement of dengue virus infection. *J Virol*. 2008;82(8):3939–3951.
38. Rodrigo WW, Jin X, Blackley SD, Rose RC, Schlesinger JJ. Differential enhancement of dengue virus immune complex infectivity mediated by signaling-competent and signaling-incompetent human Fcgamma RIA (CD64) or FcgammaRIIA (CD32). *J Virol*. 2006;80(20):10128–10138.
39. Taylor A, Foo SS, Bruzzone R, Dinh LV, King NJ, Mahalingam S. Fc receptors in antibody-dependent enhancement of viral infections. *Immunol Rev*. 2015;268(1):340–364.
40. Modhiran N, Kalayanarooj S, Ubol S. Subversion of innate defenses by the interplay between DENV and pre-existing enhancing antibodies: TLRs signaling collapse. *PLoS Negl Trop Dis*. 2010;4(12):e924.
41. Rosales C. Fcγ receptor heterogeneity in leukocyte functional responses. *Front Immunol*. 2017;8:280.
42. Guilliams M, Bruhns P, Saeys Y, Hammad H, Lambrecht BN. The function of Fcγ receptors in dendritic cells and macrophages. *Nat Rev Immunol*. 2014;14(2):94–108.
43. Tigalonowa M, Bjerke JR, Matre R. Fc gamma-receptors on Langerhans' cells and keratinocytes in suspension from normal skin characterized using soluble immune complexes and monoclonal antibodies. *Acta Derm Venereol*. 1991;71(2):99–103.
44. Nestle FO, Di Meglio P, Qin JZ, Nickoloff BJ. Skin immune sentinels in health and disease. *Nat Rev Immunol*. 2009;9(10):679–691.
45. Rathakrishnan A, et al. Cytokine expression profile of dengue patients at different phases of illness. *PLoS One*. 2012;7(12):e52215.
46. Butthep P, Chunhakan S, Yoksan S, Tangnararatchakit K, Chuansumrit A. Alteration of cytokines and chemokines during febrile episodes associated with endothelial cell damage and plasma leakage in dengue hemorrhagic fever. *Pediatr Infect Dis J*. 2012;31(12):e232–e238.
47. Yeh WT, Chen RF, Wang L, Liu JW, Shaio MF, Yang KD. Implications of previous subclinical dengue infection but not virus load in dengue hemorrhagic fever. *FEMS Immunol Med Microbiol*. 2006;48(1):84–90.

48. Boonnak K, Dambach KM, Donofrio GC, Tassaneetrithep B, Marovich MA. Cell type specificity and host genetic polymorphisms influence antibody-dependent enhancement of dengue virus infection. *J Virol*. 2011;85(4):1671–1683.
49. Vogelpoel LT, Baeten DL, de Jong EC, den Dunnen J. Control of cytokine production by human fc gamma receptors: implications for pathogen defense and autoimmunity. *Front Immunol*. 2015;6:79.
50. Halstead SB, Mahalingam S, Marovich MA, Ubol S, Mosser DM. Intrinsic antibody-dependent enhancement of microbial infection in macrophages: disease regulation by immune complexes. *Lancet Infect Dis*. 2010;10(10):712–722.
51. Collins MH, et al. Lack of durable cross-neutralizing antibodies against Zika virus from dengue virus infection. *Emerging Infect Dis*. 2017;23(5):773–781.
52. Styer LM, Lim PY, Louie KL, Albright RG, Kramer LD, Bernard KA. Mosquito saliva causes enhancement of West Nile virus infection in mice. *J Virol*. 2011;85(4):1517–1527.
53. McCracken MK, Christofferson RC, Chisenhall DM, Mores CN. Analysis of early dengue virus infection in mice as modulated by Aedes aegypti probing. *J Virol*. 2014;88(4):1881–1889.
54. Conway MJ, et al. Mosquito saliva serine protease enhances dissemination of dengue virus into the mammalian host. *J Virol*. 2014;88(1):164–175.
55. Cox J, Mota J, Sukupolvi-Petty S, Diamond MS, Rico-Hesse R. Mosquito bite delivery of dengue virus enhances immunogenicity and pathogenesis in humanized mice. *J Virol*. 2012;86(14):7637–7649.
56. Shah DK, Betts AM. Antibody biodistribution coefficients: inferring tissue concentrations of monoclonal antibodies based on the plasma concentrations in several preclinical species and human. *MAbs*. 2013;5(2):297–305.
57. Pingen M, et al. Host inflammatory response to mosquito bites enhances the severity of arbovirus infection. *Immunity*. 2016;44(6):1455–1469.
58. Payne AF, Binduga-Gajewska I, Kauffman EB, Kramer LD. Quantitation of flaviviruses by fluorescent focus assay. *J Virol Methods*. 2006;134(1-2):183–189.
59. Korkmaz E, et al. Therapeutic intradermal delivery of tumor necrosis factor-alpha antibodies using tip-loaded dissolvable microneedle arrays. *Acta Biomater*. 2015;24:96–105.
60. Cordeiro MT, et al. Results of a Zika virus (ZIKV) immunoglobulin M-specific diagnostic assay are highly correlated with detection of neutralizing anti-ZIKV antibodies in neonates with congenital disease. *J Infect Dis*. 2016;214(12):1897–1904.
61. Hristodorov D, Mladenov R, Brehm H, Fischer R, Barth S, Thepen T. Recombinant H22(scFv) blocks CD64 and prevents the capture of anti-TNF monoclonal antibody. A potential strategy to enhance anti-TNF therapy. *MAbs*. 2014;6(5):1283–1289.
62. Magalhaes T, et al. Zika virus displacement by a chikungunya outbreak in Recife, Brazil. *PLoS Negl Trop Dis*. 2017;11(11):e0006055.